Author/s:
Kang, C;Im, S;Lee, WY;Choi, Y;Stuart-Fox, D;Huertas, B

Title:
Climate predicts both visible and near-infrared reflectance in butterflies

Date:
2021-09-01

Citation:
Kang, C., Im, S., Lee, W. Y., Choi, Y., Stuart-Fox, D. & Huertas, B. (2021). Climate predicts both visible and near-infrared reflectance in butterflies. Ecology Letters, 24 (9), pp.1869-1879. https://doi.org/10.1111/ele.13821.

PROF. CHANGKU KANG (Orcid ID : 0000-0003-3707-4989)

DR. WON YOUNG LEE (Orcid ID : 0000-0002-5658-6341)

DR. DEVI STUART-FOX (Orcid ID : 0000-0003-3362-1412)

Article type : Letter

Climate predicts both visible and near-infrared reflectance in butterflies

Changku Kang[1,*], Sehyeok Im[2,3], Won Young Lee[2,*], Yunji Choi[4], Devi Stuart-Fox[5], Blanca Huertas[6]

[1]Department of Biosciences, Mopko National University, Muan, Jeollanam-do, 58554, South Korea

[2]Division of Life Sciences, Korea Polar Research Institute, Incheon, 21990, South Korea

[3]University of Science and Technology, Daejeon, 34113, South Korea

[4]Department of Life Sciences, Imperial College London, London, SW72BU, United Kingdom

[5]School of BioSciences, The University of Melbourne, Parkville, VIC 3010, Australia

[6]Department of Life Sciences, Natural History Museum London, London, SW75BD, United Kingdom

This is the author manuscript accepted for publication and has undergone full peer review but has not been through the copyediting, typesetting, pagination and proofreading process, which may lead to differences between this version and the Version of Record. Please cite this article as doi: 10.1111/ELE.13821

Running title: climate predicts butterfly reflectance

Author contributions: CK conceived the study and analysed data. CK, YC, and BH conducted museum specimen photography. SI performed image analysis. CK and WYL compiled climatic data. DSF contributed to principal ideas and phylogenetic analysis. CK prepared the initial draft of manuscript with input from WYL and DSF; all authors discussed the results and contributed to the writing of the final manuscript.

Data accessibility: Data are available at: https://datadryad.org/stash/share/1Sz0MRWiiT_tc0FnQ6-3Jf-3W3KHnLM_tq-AhMbRujg

Article type: Letters

Keywords: thermoregulation, Gloger's rule, ecogeographical patterns, Bogert's rule, thermal melanism

Number of words: 155 (abstract), 5117 (main text)

Number of references: 55

Number of figures and tables: 5 figures and 1 tables.

***Correspondence:**

Changku Kang, changku.kang@gmail.com,

C30-4130, Mopko National University, Muan, Jeollanam-do, 58554, South Korea

Tel) +82-61-450-2345, Fax) +82-61-450-2349

Won Young Lee, wonyounglee@kopri.re.kr,

Division of Life Sciences, Korea Polar Research Institute, Incheon, 21990, South Korea

Tel) +82-32-760-5523, Fax) +82-32-760-5509

Abstract

Climatic gradients frequently predict large-scale ecogeographical patterns in animal coloration, but the underlying causes are often difficult to disentangle. We examined ecogeographical patterns of reflectance among 343 European butterfly species and isolated the role of selection for thermal benefits by comparing animal-visible and near-infrared (NIR) wavebands. NIR light accounts for ~50% of solar energy but cannot be seen by animals so functions primarily in thermal control. We found that reflectance of both dorsal and ventral surfaces shows thermally

adaptive correlations with climatic factors including temperature and precipitation. This adaptive variation was more prominent in NIR than animal-visible wavebands and for body regions (thorax-abdomen and basal wings) that are most important for thermoregulation. Thermal environments also predicted the reflectance difference between dorsal and ventral surfaces, which may be due to modulation between requirements for heating and cooling. These results highlight the importance of climatic gradients in shaping the reflectance properties of butterflies at a continent-wide scale.

Introduction

Large-scale ecogeographical gradients can explain variation in diverse traits, from body size (Ashton 2002) to colour (Friedman & Remeš 2017). Several ecogeographical patterns have been formalised into rules; yet there is persistent debate regarding underlying causes and the taxa to which they apply (Gaston *et al.* 2008; Chown & Gaston 2010). This problem is epitomised by Gloger's rule and Bogert's rule, which both describe ecogeographical patterns of melanisation. Gloger's rule describes the tendency for heavily pigmented (darker) forms to be found in hotter and more humid regions (Delhey 2017, 2019). This relationship may be driven by one or more factors including camouflage in low light environments (Zink & Remsen Jr 1986; Cheng *et al.* 2018), protection from ultraviolet light or parasites (Burtt Jr & Ichida 2004; Chaplin 2004), or pleiotropic effects of genes regulating both climatic adaptations and melanin-based coloration (Ducrest *et al.* 2008). Bogert's rule (also termed the thermal melanin hypothesis) describes the tendency for darker animals to occur in colder regions because darker colours absorb more solar radiation, thus providing thermal benefits (Bogert 1949). Traditionally, Bogert's rule has been applied to ectotherms and Gloger's rule to endotherms; however, the accumulated evidence suggests that both rules may apply broadly to ectotherms or endotherms (Clusella-Trullas *et al.* 2007; Delhey 2018; Galván *et al.* 2018; Delhey *et al.* 2019). Efforts to reconcile the seemingly opposing effects of these rules have so far been hampered by the difficulty of disentangling the underlying drivers.

Most of the evidence that supports either Gloger's or Bogert's rule relates to animal-visible colour (all or part of the wavelengths range from 300–700 nm); however, the spectrum of solar irradiance extends well beyond this range. Wavelengths from 700–1400 nm (near-infrared, NIR) include approximately 50% of solar energy (Stuart-Fox *et al.* 2017) and can therefore strongly affect heat gain. By contrast, NIR does not directly affect camouflage because little or no NIR light can be seen by animals (Stuart-Fox *et al.* 2017). Examining ecogeographical gradients in NIR reflectance can therefore help to distinguish underlying drivers of ecogeographical patterns of animal coloration (Cuthill *et al.* 2017; Stuart-Fox *et al.* 2017; Ruxton *et al.* 2018). To date, large-scale ecogeographical patterns of NIR reflectance have only been examined for a limited number of taxa and a limited

geographical region (Medina *et al.* 2018; Munro *et al.* 2019).

Butterflies are a model group to investigate ecogeographical patterns of reflectance due to their thermal biology and extraordinary diversity in coloration. They are ectothermic like many insects and regulate their body temperature through both physical and behavioural traits (Clench 1966). Physical properties of the thorax and basal wings (i.e. parts of the wings that are close to thorax) directly affect the temperature of flight muscles through heat conduction (Heinrich 1974). The wings beyond the basal region may have less impact on thermoregulation because there is less haemolymph circulation and fewer vascular extensions that can carry significant quantities of heat to the thorax (Arnold 1964; Kammer & Bracchi 1973; Wasserthal 1983; Kingsolver 1987). However, wings can overheat quickly under direct sunlight due to their low thermal capacity, and butterflies have evolved sophisticated wing scale structures to control wing temperature through radiative cooling (Tsai *et al.* 2020). Butterflies also regulate their temperature through various behavioural mechanisms including dorsal (opening wings to expose dorsal surface) and lateral basking (folding wings to expose ventral surface), ground-contact, orientating themselves in relation to the position of the sun, and shivering (Clench 1966). The reflectance of butterflies plays a crucial role during behavioural thermoregulation such as dorsal and lateral basking because the efficacy of these behaviours depends on how much light their body and wings absorb (Kingsolver 1987, 1988). The reflectance of both dorsal and ventral regions seems to play a key role in warming up during basking while those of ventral regions seem to be additionally related to preventing overheating. When hot, butterflies close their wings to shield the body and high reflectance of ventral surfaces could help to prevent overheating (Kingsolver 1987). In cool environments, overheating should be less important and thus thermal pressures may act similarly on both dorsal and ventral reflectance (low dorsal-ventral contrast). In hot environments, selection for high reflectance of ventral wing surfaces to prevent overheating is predicted to produce higher dorsal-ventral contrast. However, the prediction of higher dorsal-ventral wing contrast for butterflies in hotter environments has yet to be formally tested.

In this study, we tested whether climate (mainly concerning temperature and precipitation) predicts the reflectance of both dorsal and ventral regions of 343 European butterfly species using full-spectrum photography of museum specimens. We compiled climatic niche characteristics of each species and tested multiple hypotheses regarding ecogeographical patterns of butterfly reflectance after accounting for phylogeny and phylogenetic uncertainty (Schweiger *et al.* 2014). We specifically addressed four main questions regarding ecogeographical variation in butterfly reflectance: (1) does butterfly reflectance follow the patterns predicted by Bogert's rule in both

animal-visible and near-infrared wavebands? (2) does NIR reflectance show thermally adaptive patterns independent of animal-visible reflectance? (3) does butterfly reflectance follow the patterns predicted by Gloger's rule? (4) does climate predict dorsal-ventral contrast in butterflies? Additionally, because body size has a critical role in thermoregulation and affects the efficacy of thermoregulatory behaviours (Gilchrist 1990; Kemp & Krockenberger 2004), we also tested whether body size and climatic environments have interactively shaped butterfly reflectance.

Materials and methods

Species and specimen selection

We analysed 684 butterfly specimens from 343 species held in the Lepidoptera collections at the Natural History Museum in London. This includes species from all six families, covering approximately 70 % of all species found in Europe (Wiemers *et al.* 2018). The distribution of analysed species ranged from 34° to 70° N and 10° W to 44° E. The mean temperature over a species' distribution varied from -2.7 to 18 °C, and the mean precipitation varied from 353 to 1544 mm per year. For each species, we selected and photographed two specimens whenever available and chose specimens with well-preserved wings and body. For the polymorphic species, we photographed each morph once. We focused on capturing inter- rather than intra-specific variation because we were primarily interested in evolutionary factors that have shaped broad-scale interspecific ecogeographic patterns. We note that most specimens were collected before 1980; however a previous study found no effect of specimen age on visible and near-infrared reflectance in butterflies (Munro *et al.* 2019) and any potential degradation will contribute variation within species but is unlikely to mask interspecific variation or affect biological conclusions at the scale of our analysis.

Photography

Photography was done in a dim room using two light bulbs simultaneously: an LED bulb (True-light LED 12W E27, Frankfurt, Germany CRI index 98, spectral power distributions for the bulbs are provided in Fig. S1) and a 3,000K tungsten-halogen lamp (150W, Long Life Lamp Company, Harrow, UK). The tungsten-halogen lamp emitted all ultraviolet (UV), visible, and NIR light. We set up these two bulbs approximately 60 cm above the photographic spot. A full-spectrum converted DSLR camera (Nikon D7000 converted by Lifepixel, Mukilteo, WA, USA) was set directly above the photographic area. We positioned the camera slightly below the bulbs to avoid

light reaching directly to the camera lens (Jenoptik UV-VIS-IR 60 mm 1:4 APO Macro lens; transmission waveband is between 290 to 1500 nm). We used lens filters (Baader, Mammendorf, Germany) to capture ultraviolet (U-Venus filter; transmission range from 320 to 380 nm), visible (UV/IR cut filter; 400 – 680 nm), and near-infrared wavelengths ranges (IR-Pass filter; 670 – 1050 nm; 1050 nm is the maximum sensitivity of the camera sensors provided by the manufacturer). These filters completely blocked wavelengths outside the transmission range and enabled us to photograph each specimen in three spectral ranges: ultraviolet, visible, and near-infrared ranges, respectively. Our analysed spectral range (320 – 1050 nm) captures approximately 80% of the energy in solar irradiation (Munro *et al.* 2019). Although the analysed spectral range had both small gaps (between 380 – 400 nm) and overlaps (670 – 680 nm) due to the filters' transmission ranges, their effect should be inconsequential to the overall brightness. We changed lens filters with a minimum disturbance to the camera body using a combination of magnetic lens adapters and filter holders (Manfrotto, Cassola, Italy).

To fix each specimen, we used a square paper box floored with styrofoam (17 × 10 × 5 cm). We placed each specimen at the centre with a 99% reflectance standard (WS-1-SL, Labsphere, NH, USA) on the upper-right corner of the box. Camera settings were constant (ISO 400, F8) except for the shutter speed which varied depending on the type of filters (1.3 s for ultraviolet, 1/500 s for visible, 1/800 s for near-infrared photos; different shutter speeds were used due to the different power of the light in each waveband regions). These shutter speeds ensured that the 99% reflectance standard was not saturated (i.e. pixels values exceed 255) nor seriously underexposed in all images. We photographed both dorsal and ventral sides. This produced 4,104 images saved in raw format (see Fig. S2 for sample images).

Image analysis

To remove non-linearity of the camera response, we converted all raw photos to linearised TIFF format images using Dcraw v. 9.27 (Coffin 2008). Then we rescaled each colour channel to ensure that the 99 % reflectance standard had the corresponding value. After this process, RGB values of each pixel (ranging from 0 – 255 for each colour channel) scale linearly with reflectance of 0 - 100 %. We used the B channel for UV photos, R, G, and B channels for visible photos, and R and B channels for NIR photos because the camera sensors have sensitivity in the corresponding spectral range.

For all images, we measured mean channel values of three body regions that putatively have

different role in thermoregulation: thorax-abdomen (though wing muscles are attached to thorax, abdomen is also important for thermoregulation due to haemolymph circulation between them (Rawlins 1980); we refer to thorax for brevity), basal wings, and entire wings. Thus, we measured six different body regions for each specimen: dorsal thorax (DT), dorsal basal wings (DB), dorsal entire wings (DE), ventral thorax (VT), ventral basal wings (VB), and ventral entire wings (VE). Because butterfly wings were symmetrical, we measured wing regions only from one side (left). For each region, we averaged the pixel values of all measured channels to get a mean reflectance value using ImageJ 1.52a (Schneider *et al.* 2012). Then we calculated the mean reflectance of each body part over 1) VIS (320 – 700 nm; animal-visible range), 2) NIR (700 – 1050 nm; animal-invisible near-infrared range), and 3) VIS-NIR (320 – 1050 nm) ranges. For example, VIS reflectance was calculated by $(60u + 280v)/(60 + 280)$, where u and v are the mean reflectance of ultraviolet and visible-range images respectively, and the numbers 60 and 280 are wavebands of the spectral images. We measured the entire wing area for each species (averaged among specimens) and used this as a size index for each species. Wing size is correlated with body size in butterflies but also provides a measure of the surface area exposed to sunlight.

Climatic variables

We used nine climatic niche variables for each species in our analysis. We obtained the mean, minimum, and maximum annual temperature (°C), and annual precipitation sum (mm) from an open dataset CLIMBER (Climatic niche characteristics of the butterflies in Europe) and averaged each variable across each species' distribution (data from 1971 to 2000) (Schweiger *et al.* 2014). The other five climatic variables, namely solar irradiation (kJ m^{-2} day^{-1}), isothermality, temperature seasonality, precipitation seasonality, and water vapour pressure (kPa) were compiled for every 50 km using WorldClim data (Fick & Hijmans 2017) (data from 1970 to 2000) and averaged over all years and across species' range. We chose nine variables that best represent the broad-scale climatic variation relevant to our specific hypotheses. We limited the number of variables to facilitate biological interpretation and because climatic variables tend to be very highly inter-correlated. We used annual means rather data for specific quarters because the length of the activity season varies between seasons and quarterly values are strongly correlated with annual values together with seasonality. Indeed, we extracted the mean tempearture across butterflies' distribution from April to October (flight period of most butterflies) using WorldClim datasets for each species and found that the annual mean temperature and mean temperature from April to October correlated very highly (r = 0.97).There existed one year difference between CLIMBER and WorldClim datasets due to the limitation in compiled data availability. We note here that these coarse averaged climatic variables

do not capture intra-specific variation in micro-climate conditions or altitudinal effects (which should be partially reflected in temperature variables), but should retain sufficient inter-specific variation for our large scale analysis.

Data analysis

We used R 4.0.2. for data analysis (R Core Team 2017). First, we reduced the dimensionality of the climatic variables using principal component analysis (PCA). Then we performed a phylogenetically controlled analysis to examine the relationship between size, climatic factors (PC1 and PC2; see results), and the mean butterfly reflectance over VIS-NIR range. The phylogenetic relationships of the analysed species were inferred from a published time-calibrated molecular phylogenetic tree (Wiemers *et al.* 2020). This ultrametric phylogenetic tree was based on concatenated alignment of the mitochondrial gene COI and up to eleven nuclear gene regions of European butterfly species. To account for the uncertainties in topology and node age, we generated 1,000 trees randomly sampled from the posterior distribution and performed the analysis using all 1000 trees.

For each tree, we fitted multivariate phylogenetic regressions implemented in the 'mvMORPH' package (Clavel *et al.* 2015). This enabled us to include multiple response variables in a single model. We set size, climatic principal components (PCs; up to PC2), and the interaction between size and climatic PCs as predictor variables. Our response variables consisted of the mean reflectance of the six body regions (DT, DB, DE, VT, VB, DE). We compared the goodness of fit of the models assuming either Brownian motion, Ornstein-Uhlenbeck, Early Burst, or Pagel's λ models of trait evolution and used the models with the lowest Generalized Information Criterion (GIC) (Konishi & Kitagawa 1996; Hernández *et al.* 2013). Ornstein-Uhlenbeck models showed slightly better fit than other models in multivariate phylogenetic regressions, but Pagel's λ models outperformed others in all *post-hoc* PGLS models. Thus, we consistently assumed Pagel's λ models of trait evolution. Nevertheless, the results were robust regardless of which models we assumed. We also used GIC to select the best model among all candidate models.

Using the predictors that remained significant in the above model, we performed *post-hoc* phylogenetic generalised least squares (PGLS) on the mean reflectance of each body region to further examine which body regions were specifically explained by each predictor. We implemented a 'gls' function to run PGLS (Revell 2012). We iteratively performed PGLS on 1,000 trees for all body regions and estimated the 95% confidence intervals of statistics. The 95% confidence limits of statistics from all analyses using 1000 trees varied only slightly and showed essentially the same results as the maximum clade credibility (MCC) tree results (all parameters estimated were within ±

0.02 range) supposedly because of low phylogenetic uncertainty. Thus, we report the results from the MCC tree only in the results. Here, we used Akaike Information Criteria (AIC) to select the best model and controlled for the false-discovery rate by adjusting P-values (Benjamini & Hochberg 1995). The strength of phylogenetic signal λ was estimated using the MCC tree.

We additionally examined the effects of our predictors on VIS reflectance and NIR reflectance separately using the same modelling approach and model structure. To examine whether NIR reflectance showed adaptive features even after accounting for its high correlation with VIS reflectance, we first fitted linear regressions to each NIR reflectance (for each body region) using log form of VIS reflectance as a predictor (Pearson *r* across all body regions ≈ 0.77; Fig. S3) and extracted residuals of the fitted models. These residuals indicate the degree of NIR reflectance independent of VIS reflectance (i.e. after accounting for the correlation between VIS and NIR reflectance). Though the use of residuals has been criticised due to potential for biased parameter estimation (Freckleton 2009), residuals are appropriate when the effect of one predictor on a response variable should be controlled before and independent of the other predictors such as in our case; the effects of VIS reflectance on NIR reflectance should be considered before estimating the effects of other climatic and size variables and should not affect the parameters of other predictors in the model (see Supplementary materials for the statistical justification of using residuals). We fitted multivariate phylogenetic regressions using size, climatic PCs, and the interaction between those two as predictors and the residuals for each body region as response variables. Then we performed a *post-hoc* PGLS analysis for each body region using the retained significant terms as predictors as above.

In the main results, we analysed all specimen images regardless of the sex and the presence of sexual dimorphism. However, because sexually dimorphic male reflectance is likely to be heavily shaped by sexual selection (Lande 1980; van der Bijl *et al.* 2020), we repeated the analysis without sexually dimorphic male specimens and compared the results. Furthermore, because principal components may represent a biased sample of multivariate patterns in comparative data (Uyeda *et al.* 2015), we fitted multivariate phylogenetic regressions again, but this time using the mean annual temperature and annual precipitation, instead of PC1 and PC2. We show the results of this analysis in Supplementary materials.

For the analysis of dorsal-ventral reflectance differences, we first compared the reflectance between dorsal and ventral parts using paired t-tests. Next, to examine whether climate variables predict these differences, we calculated the reflectance differences between ventral and dorsal parts by subtracting dorsal reflectance from ventral reflectance for each body region. Using these dorsal-ventral differences in the three body regions as independent variables, we fitted phylogenetic

multivariate multiple regressions with climatic PCs, size, and the interaction between them as dependent variables. We then performed *post-hoc* PGLS analyses for each body region using the retained significant terms as predictors.

Results

The overall relationship between climatic variables and VIS-NIR reflectance

Climate variables were the first two principal components (PCs) from a Principal Components Analysis (PCA) of 9 climatic niche variables. PC1 and PC2 explained 57% and 20% of the total variation, respectively. Climate PC1 was higher in species that inhabit in warmer, drier climatic conditions and correlated most strongly with mean temperature (r = 0.98), solar radiation (r = 0.88) and water vapour pressure (r = 0.87) (Fig. 1a). Climate PC2 was higher in species that inhabit areas with higher mean precipitation (r = 0.78) and low temperature seasonality (r = -0.77) (see Tables S1,2 for the full PCA results). For brevity, when reporting and discussing PC1 and PC2 effects we mainly mention temperature for PC1 and precipitation for PC2. Temperature and precipitation were the strongest correlates of PC1 and PC2 respectively and are highly correlated with the other climate variables associated with each PC.

Climate was a significant predictor of butterfly reflectance for all body regions. In the multivariate phylogenetic regression, mean total VIS-NIR reflectance was predicted by PC1 (coefficients provided in Table S3; $F_{6,334}$ = 12.58, P < 0.001), PC2 ($F_{6,334}$ = 3.66, P = 0.002), and size ($F_{6,334}$ = 7.44, P < 0.001). The two interaction variables (size×PC1 and size×PC2) were excluded from the model with P > 0.2. Phylogenetic signal was high (λ = 0.76). *Post-hoc* PGLS models that used the mean reflectance of each body region as a response variable showed that for all body regions, species from colder environments (lower PC1) had lower reflectance, which corresponded to a gradual decrease in the reflectance of butterfly assemblages across latitudinal gradients (Table 1; Figs. 2,3). PC2 was also significant for all body regions (except for the ventral thorax), with species from high precipitation environments having lower reflectance than species from drier environments. Size predicted the reflectance of both dorsal and ventral entire wing: smaller species tended to show higher mean entire wing reflectance than larger species. However, size did not predict the reflectance of either the thorax or basal wing regions (Table 1). The results from the models excluding sexually dimorphic males showed the same trends except that PC2 became non-significant for all ventral regions (Supplementary materials, Tables S4,5). Phylogenetic signals were consistently high for all body regions (all λ > 0.72).

The relationship between overall (VIS-NIR) reflectance and climate was evident for both VIS and NIR wavelength ranges but driven more by NIR reflectance for the thorax and basal wing. Results for VIS and NIR reflectance separately were essentially consistent with the overall reflectance models (see Supplementary materials, Tables S6,7, Figs. S4,5 for the full results). PC1 predicted VIS and NIR reflectance for all body regions; however, the relationship was more robust (larger coefficients) for NIR reflectance for all body regions, but not dorsal entire wing. PC2 also predicted the reflectance of most body regions except for ventral thorax and basal regions in the VIS range, and the ventral thorax in the NIR range. Size did not predict VIS reflectance of butterflies but predicted NIR reflectance of the entire wing (both dorsal and ventral); smaller butterflies showed higher NIR reflectance than larger butterflies. The direction of this relationship (i.e. whether coefficients had negative or positive values) was always the same as the overall reflectance models for all significant predictors.

We additionally examined whether NIR reflectance show adaptive variation after accounting for its high correlation with VIS reflectance (see methods). Analyses using residuals from the linear regression between NIR and log(VIS) as response variables confirmed the importance of NIR reflectance of the thorax and basal wing in the overall correlations between reflectance and climate (Table 1,2). The multivariate phylogenetic regression model showed that PC1 ($F_{6,334}$ = 4.63, P < 0.001), PC2 ($F_{6,334}$ range= 2.34, P = 0.03), and size ($F_{6,334}$ = 7.69, P < 0.001) were significant predictors of NIR residuals (Table 1). *Post-hoc* PGLS revealed that the residuals of ventral thorax and basal wing regions were higher in species from hotter environments (with higher PC1; Fig. 4). PC2 predicted dorsal thorax, basal wing, and ventral basal wing regions. Size predicted dorsal and ventral entire wing regions. The trends of the significant relationships were the same as the overall reflectance models (Table S8). All other variables were non-significant with $P_{adj} > 0.1$.

The results using the original climatic variables (the mean annual temperature and annual precipitation sum) as predictors were essentially the same as the main results except that the effect of precipitation diminished (Table S9,10). The principal component model fitted better than the original climatic variable model ($\Delta GIC \approx 10$); thus, we mainly discuss and interpret the results of the principal component model.

The relationship between climatic variables and dorsal-ventral differences

Here, we tested whether climate predicts dorsal-ventral reflectance contrast in butterflies. Ventral reflectance showed higher reflectance than dorsal reflectance for all three body regions in most of the species (all $t_{342} > 25$, $P < 0.001$, Fig. S6). Phylogenetic signal was present in these differences ($\lambda = 0.66$). In the best model, only PC1 ($F_{6,334}$ = 17.01, P < 0.001) was a significant

predictor (other terms removed with $P > 0.2$) with species from colder environments showing a greater difference between dorsal and ventral reflectance. *Post-hoc* PGLS models revealed that this relationship was present for both the thorax (*coef* = 1.47, $t = 2.63$, P_{adj}=0.01) and basal wing regions (*coef* = 1.14, $t = 4.92$, $P_{adj} < 0.001$), but not in entire wing region (*coef* = 0.00, $t = -1.42$, $P_{adj} = 0.16$).

Discussion

In this study, we analysed whether climatic variables that are related to thermal environments and precipitation explain ecogeographical patterns of butterfly reflectance. The reflectance of European butterflies followed the patterns predicted by Bogert's rule: butterfly species in colder regions showed lower reflectance than species in warmer regions in both VIS and NIR wavebands. This pattern was consistent for dorsal and ventral reflectance of all body regions. The consistent pattern for both VIS and NIR wavebands is not surprising because reflectance in these two parts of the spectrum was highly correlated. Even after removing the effect of this correlation, residual NIR reflectance of the ventral thorax-abdomen and basal wings still showed thermally adaptive patterns. Thus, our results suggest that thermal benefits drive ecogeographical patterns of reflectance in European butterflies.

The support for Gloger's rule is equivocal: the results using principal components (with a better model fit) showed patterns congruent with Gloger's rule while we found no effect of precipitation when we used annual precipitation alone as the predictor (Tables S9,10). Delhey proposed two different definitions of Gloger's rule: a simple version states that animals are darker in more humid environments while a more complex version includes differential effects of humidity and temperature on different types of melanin pigments (Delhey 2019). Our results partially follow the patterns predicted by the simple version of Gloger's rule: after accounting for the effect of temperature-related variables (PC1), reflectance of most body regions was lower in species found in more humid regions (i.e. with higher mean precipitation). The trends were consistent for all body regions (coefficients of PC2 in Tables 2 and S5-6 are all negative; although this relationship was not statistically significant for the ventral thorax). This suggests that not only thermal environments but the degree of humidity might also affect the ecogeographical patterns of butterfly reflectance. However, camouflage may also contribute to the observed relationship. Indeed, humid environments, such as closed-canopy rainforests, could favour the occurrence of darker species (Xing *et al.* 2016; Cheng *et al.* 2018), as such environments are usually covered by a dense canopy structure and thus display low light conditions.

In accordance with a previous study on Australian butterflies (Munro *et al.* 2019), we found

similar high correlations between VIS and NIR reflectance. This is not surprising because reflectance varies continuously and often gradually across the spectrum and the degree of VIS reflectance generated by pigments, such as melanins, often correlate with their NIR reflectance (Alla *et al.* 2009). However, structural colour, which is common in butterflies, can produce a wide diversity of spectral shapes with multiple peaks in different parts of the spectrum (Kinoshita *et al.* 2002), potentially enabling VIS and NIR properties to respond differently to selection. Our results suggest that selection for thermal benefits has shaped both VIS and NIR reflectance in European butterflies because both showed patterns consistent with Bogert's rule. However, the ventral basal wing and thorax regions also showed thermally-adaptive variation independent of their VIS reflectance. This implies that butterfly reflectance might be tuned to modulate signalling or camouflage needs in animal-visible wavelengths and thermoregulatory needs in NIR wavelengths despite the constraints imposed by the correlations between them (Munro *et al.* 2019).

These results are congruent with previous findings on European butterflies that analysed images in guidebooks: colour lightness of both body and wing area closest to the body increases with increasing temperature (Stelbrink *et al.* 2019). Though entire wing reflectance also showed thermally adaptive ecogeographical patterns, the strength of this relationship was weaker than for the thorax and basal wing regions. The stronger climate-reflectance relationships for the thorax and basal wing area suggest that the relative importance of thermoregulation is greater for these body regions, consistent with their more critical role in thermoregulation (Wasserthal 1983). Basal wing and thorax regions comprise a smaller area than the entire wing and are pivotal for thermoregulation due to haemolymph circulation and proximity to flight muscles (Arnold 1964), thus they may be less affected by competing selective pressures other than selection for thermal benefits. Given all this, the evolution of butterfly reflectance is likely to be affected by thermoregulation coupled with multiple competing functions, including camouflage and signalling (Silberglied 1984; Kapan 2001; Cheng *et al.* 2018; van der Bijl *et al.* 2020).

Our results show that larger species have lower entire wing reflectance than smaller species in the NIR but not VIS wavebands. In other words, size correlates with NIR reflectance, but not colour. Why have larger butterflies evolved lower NIR reflectance of the wings? NIR adaptations of wings could contribute to thermoregulation. Although heat transfer from the wings to the thorax through conduction may be limited, heat transfer may be greater for larger than smaller wings. Because larger objects have higher thermal inertia (tendency to resist changes in temperature), larger butterflies may take longer to reach flight temperature than smaller ones (Blandon *et al.* 2020). Thus, there may be stronger selection on larger butterflies to modulate NIR reflectance to reduce basking time. Alternatively, larger butterflies may prefer to be active in the shade and crepuscular hours

which could also drive the evolution of lower NIR reflectance (Xing *et al.* 2016). The underlying reason for the observed size-reflectance relationship remains to be tested.

Butterflies use both dorsal and ventral basking, and both dorsal and ventral reflectance can contribute to the process of heat transfer, depending on basking behaviour (Clench 1966; Kingsolver 1985). However, ventral regions are additionally exposed during cooling down when butterflies close their wings tightly to minimise the absorption of solar radiation (Clench 1966). To avoid the absorption of unnecessary heat during cooling down, it may be equally important to have high ventral reflectance, especially for species in warmer climates. Thus, the reflectance of ventral regions in butterflies may be a result of evolutionary modulation between two conflicting selective pressures: absorbing light energy when heating up and reflecting it when cooling down. In cold climates, selection for low reflectance to enable rapid warming may prevail, while in hot climates, there may be stronger selection for high ventral reflectance to facilitate cooling. Indeed, our results demonstrate that ventral surfaces had higher reflectance than dorsal surfaces in most species and the difference was larger in warmer climates. Notably this relationship was only present for the thorax and basal wing regions that are crucial for thermoregulation. This suggests that the evolution of the ventral surfaces of butterflies is affected by thermoregulatory pressures related to both heating and cooling.

Thermal benefits have been considered as one of the major selective agents that operate on butterfly reflectance (Kingsolver 1988; Hegna *et al.* 2013). Our findings provide the most comprehensive evidence to date that climatic gradients have shaped both animal-visible and near-infrared reflectance of butterflies consistent with both Gloger's and Bogert's rules. We also show that not all body regions were equally affected, but the observed climate-reflectance relationship was stronger for body regions that play a greater role in thermoregulation. This highlights that the relative strength of competing selective pressures (e.g. signalling, camouflage, heating up, or cooling down) may vary between different body parts and these collectively have affected the evolution of the reflectance properties of butterflies.

Acknowledgements

We are grateful to Natural History of Museum London for allowing us to photograph their invaluable specimens. We thank to A. Giusti for his help with the collections, H. Chung for his help in retrieving GPS coordinates from butterfly map images. This study was supported by National Research Foundation of Korea (grant no: NRF-2019R1C1C1002466) and Korea Polar Research Institute (grant no: PE21060). DS-F was supported by the Australian Research Council

(FT180100216).

References

Alla, S.K., Clark, J.F. & Beyette, F.R. (2009). Signal processing system to extract serum bilirubin concentration from diffuse reflectance spectrum of human skin. In: *2009 Annual International Conference of the IEEE Engineering in Medicine and Biology Society*. IEEE, pp. 1290–1293.

Arnold, J.W. (1964). Blood circulation in insect wings. *Mem. Entomol. Soc. Canada*, 96, 5–60.

Ashton, K.G. (2002). Patterns of within-species body size variation of birds: strong evidence for Bergmann's rule. *Glob. Ecol. Biogeogr.*, 11, 505–523.

Benjamini, Y. & Hochberg, Y. (1995). Controlling the false discovery rate: a practical and powerful approach to multiple testing. *J. R. Stat. Soc. Ser. B*, 57, 289–300.

van der Bijl, W., Zeuss, D., Chazot, N., Tunström, K., Wahlberg, N., Wiklund, C., *et al.* (2020). Butterfly dichromatism primarily evolved via Darwin's, not Wallace's, model. *Evol. Lett.*, 4, 545–555.

Bladon, A.J., Lewis, M., Bladon, E.K., Buckton, S.J., Corbett, S., Ewing, S.R., *et al.* (2020). How butterflies keep their cool: Physical and ecological traits influence thermoregulatory ability and population trends. *J. Anim. Ecol.*, 89, 2440–2450.

Bogert, C.M. (1949). Thermoregulation in reptiles, a factor in evolution. *Evolution*, 3, 195–211.

Burtt Jr, E.H. & Ichida, J.M. (2004). Gloger's rule, feather-degrading bacteria, and color variation among song sparrows. *Condor*, 106, 681–686.

Chaplin, G. (2004). Geographic distribution of environmental factors influencing human skin coloration. *Am. J. Phys. Anthropol.*, 125, 292–302.

Cheng, W., Xing, S., Chen, Y., Lin, R., Bonebrake, T.C. & Nakamura, A. (2018). Dark butterflies camouflaged from predation in dark tropical forest understories. *Ecol. Entomol.*, 43, 304–309.

Chown, S.L. & Gaston, K.J. (2010). Body size variation in insects: a macroecological perspective. *Biol. Rev.*, 85, 139–169.

Clavel, J., Escarguel, G. & Merceron, G. (2015). mvMORPH: an R package for fitting multivariate evolutionary models to morphometric data. *Methods Ecol. Evol.*, 6, 1311–1319.

Clench, H.K. (1966). Behavioral thermoregulation in butterflies. *Ecology*, 47, 1021–1034.

Coffin, D. (2008). DCRAW: Decoding raw digital photos in linux.

Cuthill, I.C., Allen, W.L., Arbuckle, K., Caspers, B., Chaplin, G., Hauber, M.E., *et al.* (2017). The biology of color. *Science*, 357, eaan0221.

Delhey, K. (2017). Gloger's rule. *Curr. Biol.*, 27, R689–R691.

Delhey, K. (2018). Darker where cold and wet: Australian birds follow their own version of Gloger's rule. *Ecography*, 41, 673–683.

Delhey, K. (2019). A review of Gloger's rule, an ecogeographical rule of colour: definitions, interpretations and evidence. *Biol. Rev.*, 94, 1294–1316.

Delhey, K., Dale, J., Valcu, M. & Kempenaers, B. (2019). Reconciling ecogeographical rules: rainfall and temperature predict global colour variation in the largest bird radiation. *Ecol. Lett.*, 22, 726–736.

Ducrest, A.-L., Keller, L. & Roulin, A. (2008). Pleiotropy in the melanocortin system, coloration and behavioural syndromes. *Trends Ecol. Evol.*, 23, 502–510.

Fick, S.E. & Hijmans, R.J. (2017). WorldClim 2: new 1-km spatial resolution climate surfaces for global land areas. *Int. J. Climatol.*, 37, 4302–4315.

Freckleton, R.P. (2009). The seven deadly sins of comparative analysis. *J. Evol. Biol.*, 22, 1367–1375.

Friedman, N.R. & Remeš, V. (2017). Ecogeographical gradients in plumage coloration among Australasian songbird clades. *Glob. Ecol. Biogeogr.*, 26, 261–274.

Galván, I., Rodríguez-Martínez, S. & Carrascal, L.M. (2018). Dark pigmentation limits thermal niche position in birds. *Funct. Ecol.*, 32, 1531–1540.

Gaston, K.J., Chown, S.L. & Evans, K.L. (2008). Ecogeographical rules: elements of a synthesis. *J. Biogeogr.*, 35, 483–500.

Gilchrist, G.W. (1990). The Consequences of sexual dimorphism in body size for butterfly flight and thermoregulation. *Funct. Ecol.*, 4, 475–487.

Hegna, R.H., Nokelainen, O., Hegna, J.R. & Mappes, J. (2013). To quiver or to shiver: increased melanization benefits thermoregulation, but reduces warning signal efficacy in the wood tiger moth. *Proc. R. Soc. B Biol. Sci.*, 280, 20122812.

Heinrich, B. (1974). Thermoregulation in endothermic insects. *Science*, 185, 747–756.

Hernández, C.E., Rodríguez-Serrano, E., Avaria-Llautureo, J., Inostroza-Michael, O., Morales-Pallero, B., Boric-Bargetto, D., *et al.* (2013). Using phylogenetic information and the comparative method to evaluate hypotheses in macroecology. *Methods Ecol. Evol.*, 4, 401–415.

Kammer, A.E. & Bracchi, J. (1973). Role of the wings in the absorption of radiant energy by a butterfly. *Comp. Biochem. Physiol. Part A Physiol.*, 45, 1057–1063.

Kapan, D.D. (2001). Three-butterfly system provides a field test of mullerian mimicry. *Nature*, 409, 338–340.

Kemp, D.J. & Krockenberger, A.K. (2004). Behavioural thermoregulation in butterflies: the interacting effects of body size and basking posture in *Hypolimnas bolina* (L.) (Lepidoptera:

530 Nymphalidae). *Aust J Zool*, 52, 229-239.
531 Kingsolver, J.G. (1985). Thermal ecology of Pieris butterflies (Lepidoptera: Pieridae): a new
532 mechanism of behavioral thermoregulation. *Oecologia*, 66, 540–545.
533 Kingsolver, J.G. (1987). Evolution and coadaptation of thermoregulatory behavior and wing
534 pigmentation pattern in pierid butterflies. *Evolution*, 41, 472–490.
535 Kingsolver, J.G. (1988). Thermoregulation, flight, and the evolution of wing pattern in pierid
536 butterflies: the topography of adaptive landscapes. *Am. Zool.*, 28, 899–912.
537 Kinoshita, S., Yoshioka, S. & Kawagoe, K. (2002). Mechanisms of structural colour in the *Morpho*
538 butterfly: cooperation of regularity and irregularity in an iriscedent scale. *Proc. R. Soc. B Biol.*
539 *Sci.* 269, 1417-1421.Konishi, S. & Kitagawa, G. (1996). Generalised information criteria in
540 model selection. *Biometrika*, 83, 875–890.
541 Lande, R. (1980). Sexual dimorphism, sexual selection, and adaptation in polygenic characters.
542 *Evolution*, 292–305.
543 Medina, I., Newton, E., Kearney, M.R., Mulder, R.A., Porter, W.P. & Stuart-Fox, D. (2018).
544 Reflection of near-infrared light confers thermal protection in birds. *Nat. Commun.*, 9, 3610.
545 Munro, J.T., Medina, I., Walker, K., Moussalli, A., Kearney, M.R., Dyer, A.G., *et al.* (2019).
546 Climate is a strong predictor of near-infrared reflectance but a poor predictor of colour in
547 butterflies. *Proc. R. Soc. B Biol. Sci.*, 286, 20190234.
548 R Core Team. (2017). R A Language and Environment for Statistical Computing.
549 Rawlins, J.E. (1980). Thermoregulation by the black swallowtail butterfly, Papilio polyxenes
550 (Lepidoptera: Papilionidae). *Ecology*, 61, 345–357.
551 Revell, L.J. (2012). phytools: An R package for phylogenetic comparative biology (and other things).
552 *Methods Ecol. Evol.*, 3, 217–223.
553 Ruxton, G.D., William, A.L., Sherratt, T.N. & Speed, M.P. (2018). *Avoiding attack: the evolutionary*
554 *ecology of crypsis, warning signals, and mimicry*. 2nd edn. Oxford University Press, New York.
555 Schneider, C.A., Rasband, W.S. & Eliceiri, K.W. (2012). NIH Image to ImageJ: 25 years of image
556 analysis. *Nat. Methods*, 9, 671-675.
557 Schweiger, O., Harpke, A., Wiemers, M. & Settele, J. (2014). CLIMBER: Climatic niche
558 characteristics of the butterflies in Europe. *Zookeys*, 367, 65–84.
559 Silberglied, R.E. (1984). Visual communication and sexual selection among butterflies. In: *The*
560 *Biology of Butterflies* (eds. Vane-Wright, R.I. & Ackery, P.R.). Academic Press, pp. 207–223.
561 Stelbrink, P., Pinkert, S., Brunzel, S., Kerr, J., Wheat, C.W., Brandl, R., & Zeuss, D. (2019). Colour
562 lightness of butterfly assemblages across North America and Europe. *Sci. Rep.*, 9, 1760.
563 Stuart-Fox, D., Newton, E. & Clusella-Trullas, S. (2017). Thermal consequences of colour and near-

infrared reflectance. *Philos. Trans. R. Soc. B Biol. Sci.*, 372, 20160345.

Clusella-Trullas, S., van Wyk, J.H. & Spotila, J.R. (2007). Thermal melanism in ectotherms. *J. Therm. Biol.*, 32, 235–245.

Tsai, C.-C., Childers, R.A., Nan Shi, N., Ren, C., Pelaez, J.N., Bernard, G.D., *et al.* (2020). Physical and behavioral adaptations to prevent overheating of the living wings of butterflies. *Nat. Commun.*, 11, 551.

Uyeda, J. C., Caetano, D. S., & Pennell, M. W. (2015). Comparative analysis of principal components can be misleading. *Syst. Biol.*, 64, 677-689.

Wasserthal, L.T. (1983). Haemolymph flows in the wings of pierid butterflies visualized by vital staining (Insecta, Lepidoptera). *Zoomorphology*, 103, 177–192.

Wiemers, M., Balletto, E., Dincă, V., Fric, Z.F., Lamas, G., Lukhtanov, V., *et al.* (2018). An updated checklist of the European butterflies (Lepidoptera, Papillionoidea). *Zookeys*, 811, 9–45.

Wiemers, M., Chazot, N., Wheat, C.W., Schweiger, O. & Wahlberg, N. (2020). A complete time-calibrated multi-gene phylogeny of the European butterflies. *Zookeys*, 938, 97.

Xing, S., Bonebrake, T.C., Tang, C.C., Pickett, E.J., Cheng, W., Greenspan, S.E., *et al.* (2016). Cool habitats support darker and bigger butterflies in Australian tropical forests. *Ecol. Evol.*, 6, 8062–8074.

Zink, R.M. & Remsen Jr, J. V. (1986). Evolutionary processes and patterns of geographic variation in birds. *Curr. Ornithol.*, 4, 1–69.

Table 1. Significant predictors that explain the mean reflectance of each body region from PGLS analysis on the MCC tree after controlling for the false discovery rates. Numbers in each cell show adjusted P values (see Table S3 for the coefficients). PC1 correlates positively with climatic variables including annual mean temperature, solar irradiance, and water vapour pressure. PC2 correlates positively with annual mean precipitation and negatively with temperature seasonality. D: Dorsal, V: Ventral, B: Basal wings, E: Entire wings, T: Thorax, n.s: non-significant. Significant terms are highlighted by shading.

Body region		**DT**	**DB**	**DE**	**VT**	**VB**	**VE**
Overall reflectance models (P_{adj})	**PC1**	<0.001	0.002	0.006	<0.001	<0.001	0.008
	PC2	<0.001	0.003	0.002	n.s.	0.04	0.02
	Size	n.s.	n.s.	0.005	n.s.	n.s.	0.009
Residual models (P_{adj})	**PC1**	n.s.	n.s.	n.s.	<0.001	<0.001	n.s.
	PC2	0.002	0.007	n.s.	n.s.	0.007	n.s.

	Size	n.s.	n.s.	<0.001	n.s.	n.s.	<0.001

Figure legends

Figure 1. PCA loadings on climatic factors (a) and the relationship between climatic PC1 and butterfly reflectance mapped on the butterfly phylogeny (b). The dimensionality of the six reflectance variables (mean reflectance of dorsal/ventral thorax, basal wings, and entire wings across 320 – 1050 nm range) was reduced using PCA. Reflectance PC1 explained 68% of the variation and correlated strongly with all six reflectance variables ($r > 0.71$). Colours in the phylogenetic tree indicate reflectance PC1, and colours in the heatmap show climatic PC1 (inner circle) and PC2 (outer circle).

Figure 2. Average reflectance of European butterfly species for each body region. The colour of each grid (50 × 50 km) represents the average reflectance (over 320 – 1050 nm) of all butterfly species assembly found in each grid. The colour code of each map was assigned using the Jenks natural break classification method to maximise the variance between each colour class. Red indicates that the butterfly assemblage in the area has higher reflectance while blue indicates lower reflectance ($N = 343$ species).

Figure 3. The relationship between climatic PC1 and the mean reflectance of each body region of butterflies. The trend lines represent the prediction from the multivariate phylogenetic regression models after accounting for the phylogenetic relationships.

Figure 4. The relationship between climatic PC1 and residuals of the model where near-infrared reflectance (670–1050 nm) was linearly fitted by log form of animal-visible reflectance (320–680 nm). Only ventral thorax and ventral basal wing regions showed significant trends. The trend lines represent the prediction from the PGLS models.

621 **Figure 5. The relationship between climatic PC1 and dorsal-ventral reflectance differences in**
622 **butterflies.** The difference was calculated by subtracting dorsal reflectance from ventral reflectance.
623 The trend lines represent the prediction from the multivariate phylogenetic regression models.

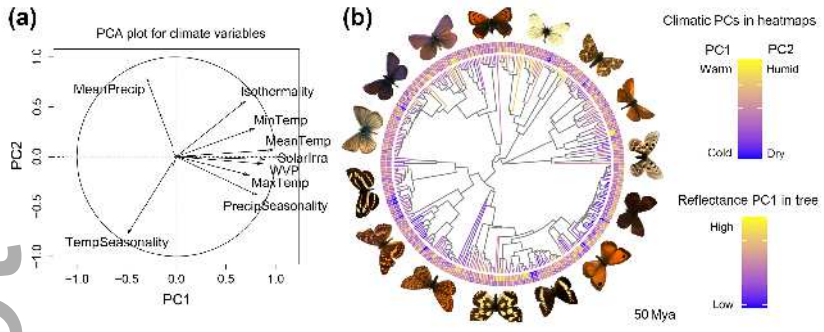

ele_13821_f1.tiff

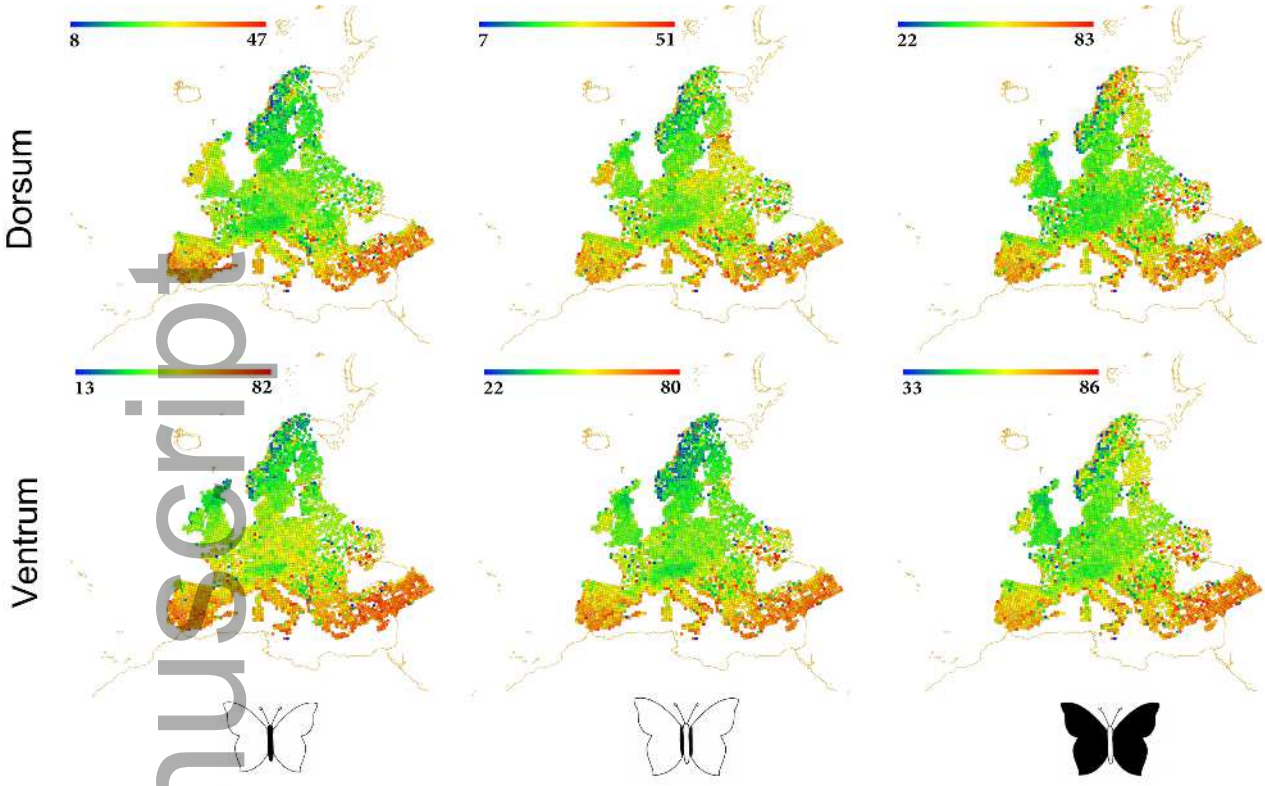

ele_13821_f2.tiff

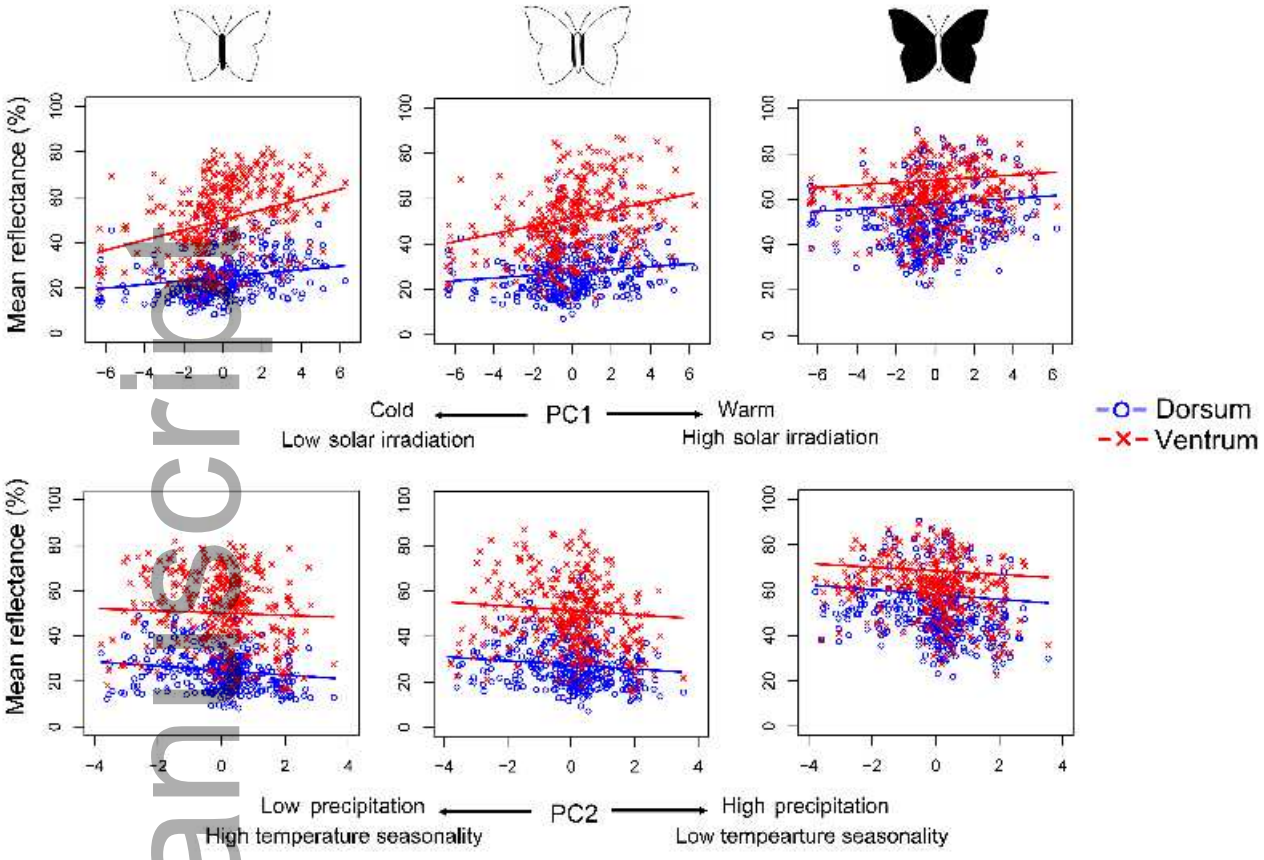

ele_13821_f3.tiff

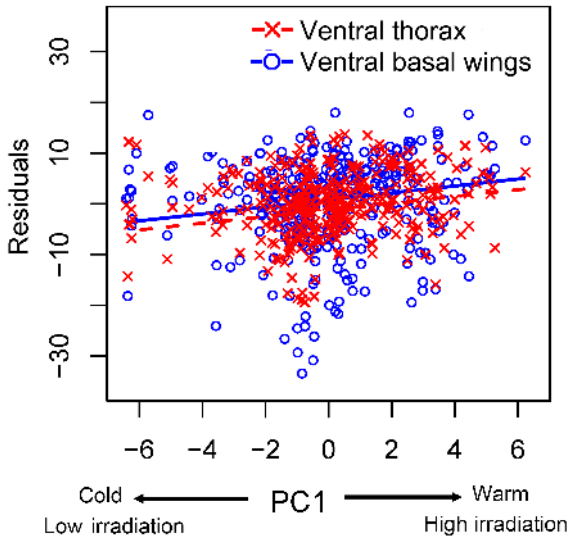

ele_13821_f4.tiff

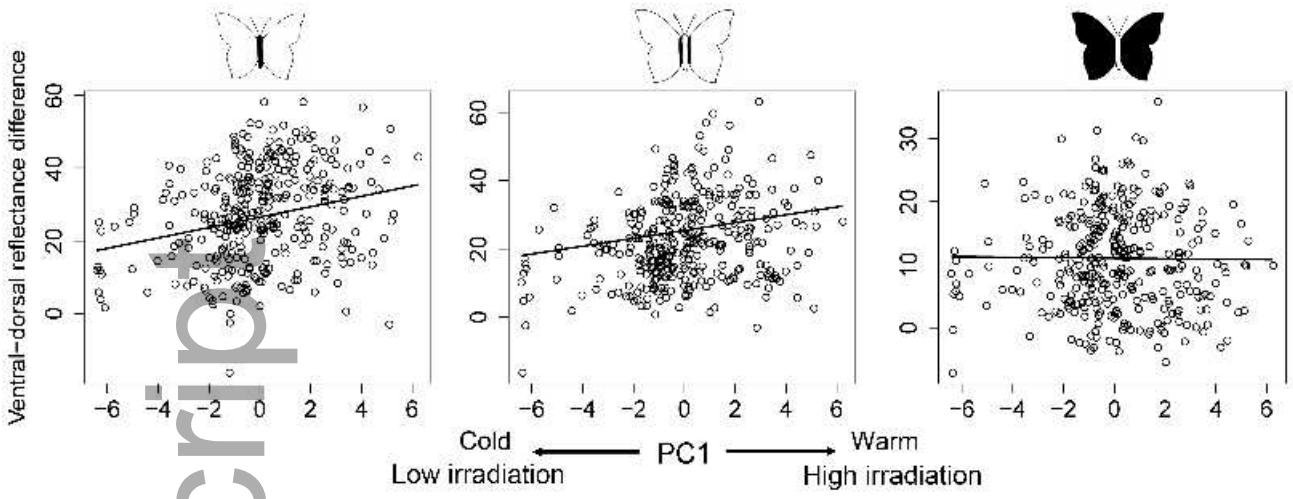

ele_13821_f5.tiff